Propagation and control of shear waves in piezoelectric composite waveguides with metallized interfaces

D G Piliposyan[1], G T Piliposian[1,2], K B Ghazaryan[3]
[1,3]Department of Dynamics of Deformable Systems and Coupled Fields,
375024 Bagramyan ave., Institute of Mechanics, Yerevan, Armenia
piliposyan@mechins.sci.am, KGhazaryan@mechins.sci.am
[2]Department of Mathematical Sciences, The University of Liverpool,
M&O Building, L69 7ZL, Liverpool, gayane@liv.ac.uk

Abstract

This paper investigates coupled electro-elastic shear waves propagating along a piezoelectric finite width waveguide consisting of layers separated by metallized interfaces and arranged in a periodic way along the guide. The modified matrix method is applied to obtain the dispersion equation for a waveguide with straight walls. Bragg resonances and the presence of trapped modes and slow waves are revealed and analysed for a periodic structure consisting of unit cells made up firstly from two different piezoelectric materials, and secondly from two identical piezoelectric materials. An analytical expression for the transmission coefficient for the waveguide with a defect layer is found that can be used to accurately detect and control the position of the passband within a stopband. This can be instrumental for constructing a tuneable waveguide made of layers of identical piezoelectric crystals separated by metallized interfaces.

Key words

Piezoelectric composite waveguide, periodic phononic crystal, bandgap, Bloch waves.

1. Introduction

Recently the problem of elastic wave propagation in piezoelectric periodic structures has been attracting increasing attention due to extensive applications in smart materials and structures, particularly those made of two or more different constituents arranged periodically. For example, thin film piezoelectric layered structures have been widely used in high frequency, high performance, small size, low cost, low energy consumption technologies.

Electro-mechanical coupling in piezoelectric materials can significantly affect the properties of acoustic waves in periodic structures and reveal new properties compared to those of purely elastic crystals. These properties have been widely discussed and investigated in one, two and three dimensional piezoelectric periodic structures (Vashishth and Gupta, 2009; Wang et al. 2009; Wilm et al. 2002; Zou et al. 2008; Yan and Wang 2008; Piliposian et al. 2012).

[1] Corresponding author

Due to the electro-mechanical coupling, piezoelectric phononic crystals become sensitive to the electric properties of the interfaces, here again exhibiting new and distinctive acoustic effects (Ghazaryan and Piliposyan, 2012; Sabina and Movchan, 2009).

Of particular interest are the properties of Bloch waves in a piezoelectric periodic waveguide. Identification of band gaps, frequencies of possible standing waves, trapped modes and slow waves in periodic piezoelectric waveguides can lead to advances in imaging devices, delay line device technologies, and the prevention and filtering of unwanted vibrations. Trapping waves due to thickness variations and mechanisms of slow waves near cut-off frequencies in an elastic waveguide have been investigated by Postnova and Craster (2007) and Craster et al. (2009). Using matrix methods these problems in in-plane and out-of-plane elasticity for waves in periodic waveguides have been studied in Adams et al. (2008) and (2009).

Piezoelectric periodic waveguides with full contact interfacial conditions have also attracted attention (Achaoui et al., 2010; Sugimoto and Makimoto, 1973; Guo et al., 2009), and in most cases the quasistatic approximation is adopted for governing equations. In some situations, however the dynamic setting of Maxwell's equations is necessary to consider when investigating the coupling resonance effects of elastic and electromagnetic waves (Piliposyan et.al, 2015). This coupling is especially important in the case of reflection/transmission problems for acoustic waves in piezoelectric materials, where acoustic and electromagnetic waves can interact strongly, and electromagnetic theory needs to be considered to give an accurate description of the reflected and transmitted waves. Such problems include coupling between the surface electromagnetic waves and elastic fields (Darinskii et al., 2008) and the reflection of quasi-normal incident plane waves (Darinskii et al., 2008, Darinskii et al. 2007).

For a piezoelectric crystal of 6mm symmetry the dynamic setting of the problem does not make the problem technically more complicated compared to the quasistatic approximation (Belubekyan, 2008). Within elasto-electrodynamic theory the propagation of SH Bloch waves in a piezoelectric waveguide with full contact interfacial conditions is considered in Piliposyan et al. (2014). The obtained analytical solutions describe both the propagation of acoustic waves and the effect of the internal resonance of electromagnetic and acoustic waves (phonon-polariton coupling), which cannot not be revealed within the quasistatic approximation.

The reflection and transmission for inclined incidence of a shear horizontal elastic wave on a stack of one dimensional piezoelectric layers made of an identical crystal with metallized interfaces is considered in Al'shits and Shuvalov (1995), where the existence of Bragg resonances is revealed and investigated. In the present paper a similar approach to that in Piliposyan et. al. (2014) is applied to obtain the analytical dispersion equation for a piezoelectric bi-material waveguide with periodically metallized interfaces. The problem is considered within

the dynamic setting of Maxwell's equations. Although for acoustic frequencies the quasistatic approximation gives a sufficiently accurate description of the problem it is not valid for "super small" incidence angles $\theta \le c_0 / c$, where c_0 and c are the sound and light velocities, and for that reason the results obtained using a quasistatic approximation do not accept the limit for the case of normal incidence (Al'shits and Shuvalov, 1995). In the present paper the case corresponding to the normal incidence is included into the analytical solution as a particular case. However, waveguides with metallized interfaces do not exhibit the acousto-optic phonon-polariton coupling demonstrated in Piliposyan et. al. (2014) for waveguides with periodic full contact interfaces.

It is also of particular interest to consider piezoelectric waveguides with a defect layer which can be introduced into the structure, and, by changing the geometry and altering the elastic characteristics of these inclusions, design tunable periodic structures (Goffaux and Vigneron, 2011). To the best of our knowledge the problem in the present setting with a defect layer has not been solved. We introduce a defect layer into the piezoelectric periodic waveguide with metallized interfaces and propose a novel tunable phononic waveguide. An analytical formula for the reflection/transmission coefficient is found which can be used to develop a tunable phononic waveguide. The problem is also investigated for a waveguide with periodically alternating boundary conditions on the waveguide walls.

2. The statement of the problem and modal expansion

In this section we obtain an analytical expression for the dispersion equation for electro-magneto-elastic coupled SH waves propagating along a finite width periodic waveguide with a unit cell of length β and occupying a region $-\infty < x < \infty, -\infty < z < \infty, \ 0 < y < h$. Each cell is made of two different hexagonal piezoelectric materials: (1) of length a_1 and (2) of length a_2 ($\beta = a_1 + a_2$) with crystallographic axes directed along the Oz direction (Fig.1).

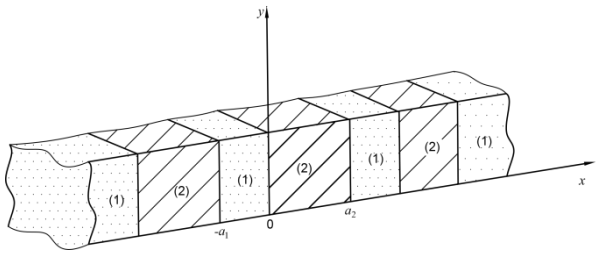

Fig. 1. Periodic waveguide with a unit cell made of two piezoelectric media.

The interconnected elastic and electro-magnetic excitations are described by the following equations and constitutive relations (Piliposian et al., 2012)

$$\frac{\partial \sigma_{ik}}{\partial x_k} = \rho \frac{\partial^2 u_i}{\partial t^2}, \tag{1}$$

$$\nabla \times \mathbf{E} = -\frac{\partial \mathbf{B}}{\partial t}, \quad \nabla \times \mathbf{H} = \frac{\partial \mathbf{D}}{\partial t}, \tag{2}$$

$$\sigma_{ij} = c_{ijkl} s_{kl} - e_{kij} E_k, \; D_i = e_{ijk} s_{jk} + \varepsilon_{ij} E_j, \tag{3}$$

where σ_{ij} is the stress tensor, ρ the mass density, u_i the displacement vector field, D_i and E_i are components of the electric displacement and electric field intensity, $\mathbf{B}$ and $\mathbf{H}$ the magnetic field induction and intensity vectors. In constitutive relations (3) c_{ijkl} is the stiffness tensor, e_{ijk} and s_{kl} the piezoelectric and strain tensors and ε_{ij} the dielectric permittivity matrix.

Harmonic time dependence, $\exp(\mathrm{i}\omega t)$ for all the physical variables with ω as a wave angular frequency is assumed henceforth. We assume that waves propagate in the (x,y) plane. Taking notation, $H_z = i\omega H$, $u_z = u$ the system of equations (1)-(3) can be reduced to the following uncoupled system of equations

$$\frac{\partial^2 u(x,y)}{\partial x^2} + \frac{\partial^2 u(x,y)}{\partial y^2} + \omega^2 \frac{\rho}{G} u(x,y) = 0, \tag{4}$$

$$\frac{\partial^2 H(x,y)}{\partial x^2} + \frac{\partial^2 H(x,y)}{\partial y^2} + +\omega^2 \varepsilon_{11} \mu_{33} H(x,y) = 0, \tag{5}$$

and constitutive relations expressed via $H(x,y)$ and $u(x,y)$

$$E_y = -\frac{e_{15}}{\varepsilon_{11}} \frac{\partial u}{\partial y} + \frac{1}{\varepsilon_{11}} \frac{\partial H}{\partial x}, \; E_x = -\frac{e_{15}}{\varepsilon_{11}} \frac{\partial u}{\partial x} - \frac{1}{\varepsilon_{11}} \frac{\partial H}{\partial y}, \tag{6}$$

$$\sigma_{xz} = G \frac{\partial u}{\partial x} + \frac{e_{15}}{\varepsilon_{11}} \frac{\partial H}{\partial y}, \; \sigma_{yz} = G \frac{\partial u}{\partial y} - \frac{e_{15}}{\varepsilon_{11}} \frac{\partial H}{\partial x}, \tag{7}$$

where $G = c_{44} + \frac{e_{15}^2}{\varepsilon_{11}}$. Dimensionless coordinates $x = \tilde{x}h$ and $y = \tilde{y}h$ will be introduced and the tilde sign will be omitted henceforth. Two types of boundary conditions on the waveguide walls will be considered:

1. Displacement-clamped and electrically-shorted

$$u(x,0) = 0, \qquad E_x(x,0) = 0, \quad u(x,1) = 0, \quad E_x(x,1) = 0. \tag{8}$$

2. Traction free $\sigma_{yz}(x,0) = 0$, $\sigma_{yz}(x,1) = 0$ and electrically open, which, due to the equality $\partial H(x,y)/\partial x = -D_y(x,y)$ is equivalent to $H(x,0) = 0, \; H(x,1) = 0.$ (9)

The solution of (4)-(5) can be written as $(u(x,y), H(x,y)) = (u(y), H(y))(\mathrm{e}^{\mathrm{i}qx}, \mathrm{e}^{\mathrm{i}sx})$ leading to an eigenvalue problem with discrete eigenvalues q_n and s_n, and corresponding mode solutions $(u_n(x,y), H_n(x,y))$ with

$$u_n(x,y) = a_n(x) r_n(y), \; H_n(x,y) = ec_n(x) z_n(y), \tag{10}$$

$$E_{yn}(x,y)=\eta v_n(x)z_n(y),\quad \sigma_{xzn}(x,y)=Gw_n(x)r_n(y), \tag{11}$$

$$r_n(y)=\begin{cases}\sin(p_n y)\\ \cos(p_n y)\end{cases},\qquad z_n(y)=\begin{cases}\cos(p_n y)\\ \sin(p_n y)\end{cases}, \tag{12}$$

where $e=e_{15}$ and is included in the expression of $H_n(x,y)$ to harmonise the dimensions of all the wave-field functions and

$$w_n(x)=\left[q_n b_n(x)+(-1)^i\theta p_n c_n(x)\right],\ v_n(x)=\left[(-1)^i p_n a_n(x)+s_n d_n(x)\right],\ i=1,2, \tag{13}$$

$$\eta=\frac{e}{\varepsilon},\ \theta=\frac{e^2}{G\varepsilon},\quad q_n=\sqrt{\frac{\omega^2h^2}{c_0^2}-p_n^2},\quad s_n=\sqrt{\frac{\omega^2h^2}{c^2}-p_n^2}, c_0=\sqrt{\frac{G}{\rho}}, c=\sqrt{\frac{1}{\mu\varepsilon}}, \tag{14}$$

c_0 is the velocity of a transverse wave in the medium, c is the speed of the electromagnetic wave, $i=1,2$ correspond to the upper and lower terms in (12) with $p_n=\pi n$ and $p_n=\pi(n-1)$, $n=0,1,2\ldots$ respectively, corresponding to solutions for boundary conditions (8) and (9), and the following notations are introduced within a homogeneous material (Piliposyan et al., 2014)

$$\begin{aligned}a_n(x)&=A_n\exp(iq_n x)+B_n\exp(-iq_n x),\quad b_n(x)=i\left(A_n\exp(iq_n x)-B_n\exp(-iq_n x)\right),\\ c_n(x)&=C_n\exp(is_n x)+D_n\exp(-is_n x),\quad d_n(x)=i\left(C_n\exp(is_n x)-D_n\exp(-is_n x)\right),\end{aligned} \tag{15}$$

where $A_n\exp(iq_n x)$ and $C_n\exp(is_n x)$ correspond to forward propagating, $B_n\exp(-iq_n x)$ and $D_n\exp(-is_n x)$ reflected waves and A_n, B_n, C_n, D_n are constants.

2.1 Solution for a periodic piezoelectric waveguide with metallized interfaces

The boundary conditions between two different homogeneous materials at the interfaces $x=0$ and $x=a_2$ are continuity conditions for the displacement and the normal stresses

$$\begin{pmatrix}u^{(1)}(x)\\ \sigma_{xz}^{(1)}(x)\end{pmatrix}=\begin{pmatrix}u^{(2)}(x)\\ \sigma_{xz}^{(2)}(x)\end{pmatrix}, \tag{16}$$

and, since the layers are separated by thin metallized coatings, zero electrical field at both sides of the interfaces (Fig 1)

$$E_y^{(1)}(x)=0,\ E_y^{(2)}(x)=0 \tag{17}$$

Using (11)-(13) these conditions can be written as

$$\sum_n\begin{pmatrix}a_n^{(1)}(x)r_n^{(1)}(y)\\ G^{(1)}w_n^{(1)}(x)r_n^{(1)}(y)\end{pmatrix}=\sum_n\begin{pmatrix}a_n^{(2)}(x)r_n^{(2)}(y)\\ G^{(2)}w_n^{(2)}(x)r_n^{(2)}(y)\end{pmatrix}, \tag{18}$$

$$v_n^{(1)}(x)=0,\qquad v_n^{(2)}(x)=0, \tag{19}$$

where the superscripts 1,2 indicate the first and second material respectively.

An inner product can be defined as

$$\langle r_m(y) \mid r_n(y) \rangle = \int_0^h r_m(y) r_n(y) dy \,, \tag{20}$$

which has an orthogonality feature within the same material. Taking the inner product of (18) with a single mode *m* gives

$$\begin{pmatrix} a_n^{(1)}(x) L_{nm} \\ w_n^{(1)}(x) L_{nm} \end{pmatrix} = \begin{pmatrix} a_m^{(2)}(x) \hat{\mathrm{I}} \\ \gamma w_n^{(2)}(x) \hat{\mathrm{I}} \end{pmatrix}, \tag{21}$$

where $L_{mn} = \int_0^1 r_n^{(1)}(y) r_m^{(2)}(y) dy$, $(n, m = 1, 2, 3\ldots)$.

When the wave characteristics are continuous, the transfer matrix coupling the wave fields in neighboring cells can be constructed directly by joining the wave fields at the interfaces (Piliposian et al., 2012). The transfer matrix in the case of electrically shorted boundary conditions (19) is not possible to construct since in this case the interface matrices are degenerate and impossible to invert. In this case using (19) the amplitudes $c_n^{(i)}(x)$ and $d_n^{(i)}(x)$ can be eliminated from (21) and the transfer matrix can be modified and written in terms of the vectors $\mathbf{a}^{(j)} = \left[a_n^{(j)}(x) \right]_{n=1,2,\ldots N}$ and $\mathbf{b}^{(j)} = \left[b_n^{(j)}(x) \right]_{n=1,2,\ldots,N}$ in the following way:

$$\hat{\mathrm{N}}_1 \begin{pmatrix} \mathbf{a}^{(1)}(0) \\ \mathbf{b}^{(1)}(0) \end{pmatrix} = \hat{\mathrm{N}}_2 \begin{pmatrix} \mathbf{a}^{(2)}(0) \\ \mathbf{b}^{(2)}(0) \end{pmatrix}, \hat{\mathrm{R}}_1 \begin{pmatrix} \mathbf{a}^{(1)}(a_2) \\ \mathbf{b}^{(1)}(a_2) \end{pmatrix} = \hat{\mathrm{R}}_2 \begin{pmatrix} \mathbf{a}^{(2)}(a_2) \\ \mathbf{b}^{(2)}(a_2) \end{pmatrix}, \tag{22}$$

with

$$\hat{\mathrm{N}}_1 = \begin{pmatrix} \hat{\mathrm{L}}, & 0 \\ \hat{\mathrm{L}}\hat{\mathrm{V}}^{(1)}, & \hat{\mathrm{L}}\hat{\mathrm{Q}}^{(1)} + \hat{\mathrm{L}}\hat{\mathrm{W}}^{(1)} \end{pmatrix}, N_2 = \begin{pmatrix} \hat{\mathrm{I}}, & 0 \\ -\gamma\hat{\mathrm{V}}^{(2)}, & \gamma\hat{\mathrm{Q}}^{(2)} + \gamma\hat{\mathrm{W}}^{(2)} \end{pmatrix},$$

$$\hat{\mathrm{R}}_1 = \begin{pmatrix} \hat{\mathrm{L}}, & 0 \\ -\hat{\mathrm{L}}\hat{\mathrm{V}}^{(1)}, & \hat{\mathrm{L}}\hat{\mathrm{Q}}^{(1)} + \hat{\mathrm{L}}\hat{\mathrm{W}}^{(1)} \end{pmatrix}, \hat{\mathrm{R}}_2 = \begin{pmatrix} \hat{\mathrm{I}}, & 0 \\ \gamma\hat{\mathrm{V}}^{(2)}, & \gamma\hat{\mathrm{Q}}^{(2)} + \gamma\hat{\mathrm{W}}^{(2)} \end{pmatrix}, \tag{23}$$

where matrices $\hat{\mathrm{Q}}^{(j)}$, $\hat{\mathrm{V}}^{(j)}$ and $\hat{\mathrm{W}}^{(j)}$ have elements

$$V_{mn}^{(j)} = \left(p_n^{(j)} \right)^2 \frac{\theta^{(j)} \left(\cos\left(a_j s_n^{(j)} \right) - \cos\left(a_j q_n^{(j)} \right) \right)}{\mathrm{s}_n^{(j)} \sin(a_j s_n^{(j)})} \delta_{mn}, W_{mn}^{(j)} = \left(\left(p_n^{(j)} \right)^2 \frac{\theta^{(j)}}{s_n^{(j)}} \frac{\sin(a_j q_n^{(j)})}{\sin(a_j s_n^{(j)})} \right) \delta_{mn},$$

$$Q_{mn}^{(j)} = q_n^{(j)} \delta_{nm}, \qquad \gamma = \frac{G_2}{G_1}, \tag{24}$$

$\hat{\mathrm{I}}$ is an identity matrix and δ_{mn} is the Kronecker delta operator.

Writing the Bloch-Floquet conditions as

$$\exp(\mathrm{i}k\beta) \left(\mathbf{a}^{(1)}(-a_1), \mathbf{b}^{(1)}(-a_1) \right)^T = \left(\mathbf{a}^{(1)}(a_2), \mathbf{b}^{(1)}(a_2) \right)^T,$$

where k is the Bloch wave number, and using the transfer matrices (23) across the interfaces, the problem can be written in the following form

$$\exp(\mathrm{i}k\beta) \begin{pmatrix} \mathbf{a}^{(1)}(-a_1) \\ \mathbf{b}^{(1)}(-a_1) \end{pmatrix} = \left(\hat{\mathrm{R}}_1^{-1} \hat{\mathrm{R}}_2 \right) \hat{\mathrm{T}}^{(2)}(0) \left(\hat{\mathrm{N}}_2^{-1} \hat{\mathrm{N}}_1 \right) \hat{\mathrm{T}}^{(1)}(-a_1) \begin{pmatrix} \mathbf{a}^{(1)}(-a_1) \\ \mathbf{b}^{(1)}(-a_1) \end{pmatrix}, \tag{25}$$

where

$$\hat{\mathrm{T}}^{(j)}(x') = \begin{pmatrix} \hat{\mathrm{C}}_{q_n}^{(j)} & \hat{\mathrm{S}}_{q_n}^{(j)} \\ -\hat{\mathrm{S}}_{q_n}^{(j)} & \hat{\mathrm{C}}_{q_n}^{(j)} \end{pmatrix}, \tag{26}$$

is the transfer matrix within a homogeneous material, and $\hat{\mathrm{C}}_{q_n}^{(j)}$ and $\hat{\mathrm{S}}_{q_n}^{(j)}$ are $N \times N$ matrices with entries $\cos(q_n^{(j)}(x'-x))$ and $\sin(q_n^{(j)}(x'-x))$ along the main diagonal.

For homogeneous boundary conditions on the guide walls the matrix $\hat{\mathrm{L}}$ in (23) becomes an identity matrix, the propagating modes separate from each other and each gives rise to the following dispersion equation (Ghazaryan and Piliposyan, 2012)

$$\cos(k\beta) = -\frac{f(p,\omega)}{g(p,\omega)}, \tag{27}$$

$$f(p,\omega) = A + Q_1 Q_2 P + Q_1 R_1 + Q_2 R_2, \quad g(p,\omega) = (1+Q_1)(1+Q_2),$$

where

$$R_{1,2} = \cos\left(a_{1,2}q^{(1,2)}\right)\cos\left(a_{2,1}s^{(2,1)}\right) + \frac{e^{(2,1)^2}\varepsilon^{(1,2)}q^{(1,2)}}{e^{(1,2)^2}\varepsilon^{(2,1)}q^{(2,1)}}\frac{\sin\left(a_{1,2}q^{(1,2)}\right)}{\sin\left(a_{2,1}q^{(2,1)}\right)}\left(\cos\left(a_{2,1}q^{(2,1)}\right)\cos\left(a_{1,2}s^{(1,2)}\right)-1\right),$$

$$A = \cos\left(a_1 q^{(1)}\right)\cos\left(a_2 q^{(2)}\right) - \frac{(G^{(1)^2}q^{(1)^2} + G^{(2)^2}q^{(2)^2})}{2q^{(1)}q^{(2)}G^{(1)}G^{(2)}}\sin\left(a_1 q^{(1)}\right)\sin\left(a_2 q^{(2)}\right),$$

$$P = \left(\cos\left(a_1 q^{(1)}\right)\cos\left(a_2 q^{(2)}\right) - \frac{q^{(1)^2}e^{(2)^4}\varepsilon^{(1)^2} + q^{(2)^2}e^{(1)^4}\varepsilon^{(2)^2}}{2e^{(1)^2}e^{(2)^2}q^{(1)}q^{(2)}\varepsilon^{(1)}\varepsilon^{(2)}}\sin\left(a_1 q^{(1)}\right)\sin\left(a_2 q^{(2)}\right)\right),$$

$$Q_{1,2} = \frac{p^2 e^{(1,2)^2}\sin\left(a_{1,2}s^{(1,2)}\right)}{G^{(1,2)}\varepsilon^{(1,2)}q^{(1,2)}s^{(1,2)}\sin\left(a_{1,2}q^{(1,2)}\right)},$$

$$e^{(j)} = e_{15}^{(j)}, \quad \varepsilon^{(j)} = \varepsilon_{11}^{(j)}, \quad \mu^{(j)} = \mu_{33}^{(j)}, \qquad j = 1,2.$$

Without the piezoelectric effect equation (27) will describe the propagation of the acoustic wave in the periodic waveguide with the dispersion equation $\cos(k\beta) = A$.

Dispersion equation (27) is the same both for displacement-clamped and electrically-shorted (8), and traction free and magnetically-closed boundary conditions (9) on the waveguide walls. In the case of boundary condition (8) mode $n = 0$, corresponding to the normal incidence, leads to a trivial solution for the displacement and the electromagnetic field independent of y, $H(x,y) = H(x)$ which due to electrically shorted interface conditions leads to no wave propagation. In the case of boundary condition (9) mode $n = 0$ leads to a solution for the displacement that is independent of y, $u(x,y) = u(x)$, and a trivial solution for the electromagnetic field function, giving the propagation only of an acoustic wave described by the dispersion equation $\cos(k\beta) = A$ with the piezoelectric effect present only in the piezoelectrically stiffened elastic modulus G.

For a superlattice with cells composed of two identical piezoelectric materials ($e_1 = e$, $e_2 = e$) of equal widths $a_2 = a_1 = a$, the dispersion equation (27) takes the following form:

$$\cos(ak)=\frac{\cos(aq)\sin(as)+\eta\cos(as)\sin(aq)}{\sin(as)+\eta\sin(aq)},\ \eta=\frac{\theta p^2}{qs}, \qquad (28)$$

where the parameters q and s are expressed by formulae (14) without indices. It is clear from (28) that for electrically shorted interfaces between two constituent materials in the waveguide band gaps are possible if these materials are identical. In this case however the opposite polarization will not affect the band structure.

3. Reflection/Transmission of acoustic waves in a piezoelectric waveguide with finite stacks

In this section we investigate the reflection/transmission properties of a finite stack of cells in a piezoelectric waveguide by coupling the wave fields in neighboring layers via a matrix propagator. We consider a structure consisting of a stack of M cells, each containing a pair of layers a_j, (j= 1,2) made from different piezoelectric crystals and one additional single layer, thus 2M+1 layers altogether (Fig. 1). On each side the waveguide has two infinite piezoelectric substrates made from material 2.

For continuity of wave fields between layers the matrix propagator can be constructed directly. The electrically shorted case however cannot be obtained from this as a particular case since the amplitudes at interfaces will become connected via degenerate matrices which cannot be inverted. To get around this problem electrically shorted boundary conditions (17) at the interfaces $x=m\beta+a_1$ between two layers (m,1) and (m,2) (the same at the interface (m,2) and (m+1,1)) can be incorporated into the continuity boundary conditions for displacements and stresses (16) (Al'shits and Shuvalov,1995).

From (4)-(7) the complete magneto-elastic wave field in the m^{th} cell is

$$\begin{pmatrix} u_{(m)}(x)\\ \sigma_{xz(m)}(x)\\ H_{(m)}(x)\\ E_{y(m)}(x)\end{pmatrix}=A\begin{pmatrix}1\\ \mathrm{i}Gq\\ 0\\ ep/\varepsilon\end{pmatrix}e^{\mathrm{i}q(x-m\beta)}+B\begin{pmatrix}1\\ -\mathrm{i}Gq\\ 0\\ ep/\varepsilon\end{pmatrix}e^{-\mathrm{i}q(x-m\beta)}+C\begin{pmatrix}0\\ -e^2p/\varepsilon\\ 1\\ -\mathrm{i}e^2s/\varepsilon\end{pmatrix}e^{\mathrm{i}s(x-m\beta)}+D\begin{pmatrix}0\\ -e^2p/\varepsilon\\ 1\\ \mathrm{i}e^2s/\varepsilon\end{pmatrix}e^{-\mathrm{i}s(x-m\beta)}, \qquad (29)$$

where the factor $\exp(\mathrm{i}(py-\omega t))$ is omitted and all the parameters apart from p have superscripts (j) which are also omitted, (j=1,2) correspond to the material number in the unit cell. We will investigate the transmission properties of only acoustic waves since the piezoelectric effect does not have a noticeable effect on electromagnetic waves. From (29) and (17) the amplitudes $C^{(j)}$ and $D^{(j)}$ in the expression for $E_y^{(j)}$ can be expressed via the amplitudes $A^{(j)}$ and $B^{(j)}$ in the following way

$$\begin{pmatrix}C^{(1)}\\ D^{(1)}\end{pmatrix}=\begin{pmatrix}\eta_+^{(1)}e^{\mathrm{i}a_1(s^{(1)}-q^{(1)})} & \eta_-^{(1)}e^{\mathrm{i}a_1(s^{(1)}+q^{(1)})}\\ -\eta_-^{(1)} & -\eta_+^{(1)}\end{pmatrix}\begin{pmatrix}A^{(1)}\\ B^{(1)}\end{pmatrix},$$

$$\begin{pmatrix} C^{(2)} \\ D^{(2)} \end{pmatrix} = \begin{pmatrix} \eta_+^{(2)} e^{i\beta(s^{(2)}-q^{(1)})} & \eta_-^{(2)} e^{i\beta(s^{(2)}+q^{(1)})} \\ -\eta_-^{(2)} e^{-ia_1(s^{(2)}+q^{(1)})} & -\eta_+^{(2)} e^{-ia_1(s^{(2)}-q^{(1)})} \end{pmatrix} \begin{pmatrix} A^{(2)} \\ B^{(2)} \end{pmatrix}, \ \eta_\pm^{(j)} = \frac{ip(1-e^{ia_j(s^{(j)}\pm q^{(j)})})}{s^{(j)}(e^{2ia_j s^{(j)}}-1)} \ . \quad (30)$$

The amplitudes $C^{(j)}$ and $D^{(j)}$ will be eliminated by substituting (30) into the expression for $\sigma_{xz}^{(j)}(x)$ in the boundary conditions (16). Formula (16) will have only the incident and reflected amplitudes $A^{(j)}$ and $B^{(j)}$ of a coupled magneto-elastic wave. Then a 2×2 unimodular transfer matrix $\hat{\mathrm{S}}$ coupling the amplitudes of forward and backward travelling waves $A_m^{(1)}$ and $B_m^{(1)}$ in layers made from material 1 in the two neighbouring cells (m) and (m+1) can be constructed s uch that

$$\begin{pmatrix} A_m^{(1)} \\ B_m^{(1)} \end{pmatrix} = \hat{\mathrm{S}} \begin{pmatrix} A_{m+1}^{(1)} \\ B_{m+1}^{(1)} \end{pmatrix}, \quad (31)$$

where

$$\hat{\mathrm{S}} = \hat{\mathrm{S}}^{(1)} \hat{\mathrm{S}}^{(2)} \ ,$$

the elements of matrices $\hat{\mathrm{S}}^{(1)}$ and $\hat{\mathrm{S}}^{(2)}$ are

$$S_{11}^{(1)} = S_{22}^{(1)*} = e^{-i\beta q^{(2)}} \frac{(\psi_+^{(1)}-1)+\gamma(\psi_+^{(2)}-1)}{\psi_+^{(1)}-\psi_-^{(1)}-2}, \ S_{12}^{(1)} = S_{21}^{(1)*} = \mathrm{e}^{i\beta q^{(2)}} \frac{(\psi_+^{(1)}-1)+\gamma(\psi_-^{(2)}+1)}{\psi_+^{(1)}-\psi_-^{(1)}-2}, \quad (32)$$

$$S_{11}^{(2)} = S_{22}^{(2)*} = e^{-ia_1\left(q^{(1)}-q^{(2)}\right)} \frac{(\psi_+^{(1)}-1)+\gamma(\psi_+^{(2)}-1)}{\gamma(\psi_+^{(2)}-\psi_-^{(2)}-2)} \ , \ S_{12}^{(2)} = S_{21}^{(2)*} = e^{ia_1\left(q^{(1)}+q^{(2)}\right)} \frac{(\psi_-^{(1)}+1)+\gamma(\psi_+^{(2)}-1)}{\gamma(\psi_+^{(2)}-\psi_-^{(2)}-2)}, \quad (33)$$

$$\psi_\pm^{(j)} = \chi^{(j)} \frac{1-2\mathrm{e}^{ia_j(s^{(j)}\pm q^{(j)})}+e^{2ia_j s^{(j)}}}{e^{2ia_j s^{(j)}}-1}, \ \chi^{(j)} = \frac{p^2\theta^{(j)}}{q^{(j)}s^{(j)}} \ , \quad (34)$$

and * in the superscript denotes the complex conjugate. The amplitudes of the incident A_I, reflected B_R and transmitted A_T acoustic waves in the two substrates will thus have the relation

$$\begin{pmatrix} A_I \\ B_R \end{pmatrix} = \hat{\mathrm{S}}^M \begin{pmatrix} A_T \\ 0 \end{pmatrix}. \quad (35)$$

Using Sylvester's theorem for a 2×2 unimodular matrix, the matrix $\hat{\mathrm{S}}^M$ can be written as

$$\hat{\mathrm{S}}^M = \begin{pmatrix} S_{11} & S_{12} \\ S_{12}^* & S_{11}^* \end{pmatrix}^M = \begin{pmatrix} S_{11}U_{M-1}-U_{M-2} & S_{12}U_{M-1} \\ S_{12}^*U_{M-1} & S_{11}^*U_{M-1}-U_{M-2} \end{pmatrix}, \quad (36)$$

where $$U_M = \frac{\sin((M+1)k\beta)}{\sin(k\beta)},$$

and where the Bloch wave number k is defined by the equation

$$\cos(k\beta) = (S_{11}+S_{11}^*)/2 \, . \quad (37)$$

From (35) and (36) the reflection/transmission problem can be written as

$$\begin{pmatrix} A_I \\ B_R \end{pmatrix} = \begin{pmatrix} S_{11}U_{M-1} - U_{M-2} & S_{12}U_{M-1} \\ S_{12}^{*}U_{M-1} & S_{11}^{*}U_{M-1} - U_{M-2} \end{pmatrix} \begin{pmatrix} A_T \\ 0 \end{pmatrix}. \tag{38}$$

From (38) we find that the reflection coefficient is

$$R = \frac{B_R}{A_I} = \frac{\mathrm{S}_{12}^{*}U_{M-1}}{\mathrm{S}_{11}U_{M-1} - U_{M-2}}\ , \tag{39}$$

and

$$|R|^2 = \frac{|S_{12}|^2}{|S_{12}|^2 + (\sin(k\beta)/\sin(M\,k\beta))^2}\ . \tag{40}$$

For $p = 0$, corresponding to a normal incidence, the reflection coefficient R takes the following form

$$|R|^2 = \frac{1}{4}\left(\sqrt{\frac{G^{(2)}\rho^{(2)}}{G^{(1)}\rho^{(1)}}} - \sqrt{\frac{G^{(1)}\rho^{(1)}}{G^{(2)}\rho^{(2)}}}\right)^2 \sin^2\left(\frac{\omega a_2}{c_0^{(2)}}\right),$$

which shows that in this case there would be a total transmission for the piezoelectric waveguide with identical piezoelectric materials.

At the band edges, where $k\beta = \pi n$, the reflectivity will be given by

$$|R|^2 = \frac{|S_{12}|^2}{|S_{12}|^2 + (1/M)^2}\ , \tag{41}$$

and the transmissivity by

$$|T|^2 = 1 - |R|^2.$$

Within the band gaps, where $k\beta$ is complex, $k\beta = \pi n + \mathrm{i}\delta$, formula (40) takes the form

$$|R|^2 = \frac{|S_{12}|^2}{|S_{12}|^2 + (\sinh(\delta)/\sinh(M\delta))^2}\ . \tag{42}$$

It follows from (42) that the reflection coefficient will approach unity as the number of cells increases and the total reflection regions will precisely coincide with the stopband for Bloch waves.

3.1 *Transmission coefficient in the piezoelectric composite waveguide with a defect layer*

We now introduce a defect layer Z as shown in Fig.2, such that the waveguide has a mirror symmetry about this layer.

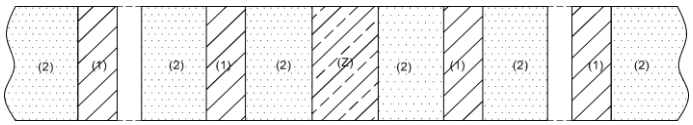

Fig. 2. Finite stack piezoelectric waveguide between two infinite substrates and a defect layer.

The transfer matrix now will have the following form:

$$\begin{pmatrix} A_I \\ B_R \end{pmatrix} = \hat{\mathrm{S}}^M \hat{\mathrm{Z}}\, \hat{\mathrm{S}}^M \begin{pmatrix} A_T \\ 0 \end{pmatrix}, \tag{43}$$

where $\hat{\mathrm{Z}} = \hat{Z}^{(1)}\hat{Z}^{(2)}$, and the elements of the matrices $Z^{(1)}$ and $Z^{(2)}$ can be obtained from the elements of the matrices $\hat{\mathrm{S}}^{(1)}$ and $\hat{\mathrm{S}}^{(2)}$ by changing the material parameters of the second material in (32)-(34) to those of the defect layer. The Sylvester's theorem can be used to obtain an expression for the transmission coefficient

$$T = \frac{A_T}{A_I} = \frac{1}{Z_{11}U_{M-2}^2 - Z_2 U_{M-2}U_{M-1} + Z_3 U_{M-1}^2}\ , \tag{44}$$

is the transfer matrix through the defect layer and the following notations are introduced

$$Z_2 = 2S_{11}Z_{11} + S_{12}^* Z_{12} + S_{12}Z_{12}^*,$$

$$\mathrm{Z}_3 = |\, S_{12}\,|^2 Z_{11}^* + S_{11}\left(Z_2 - S_{11}Z_{11}\right).$$

The analytical expression (44) for the transmission coefficient can be used to investigate the defect mode in a waveguide with a finite stack of cells, each cell composed of either two different or two identical piezoelectric materials.

4. Discussion

4.1 Homogeneous boundary conditions on the guide walls the matrix

Numerical calculations have been carried out for two piezoelectric phononic crystals. Material parameters of PZT-4 and BaTiO3 have been used for one phononic crystal and PZT-4 for the piezoelectric waveguide with identical layers (Table 1). For homogeneous boundary conditions on the guide walls the results are the same both for displacement-clamped and electrically-shorted (8), and traction free and magnetically-closed boundary conditions (9) on the waveguide walls.

Table 1. Material constants of PZT-4, $LiIO_3$ and $BaTiO_3$

Material	Elastic constant $c_{44}\cdot 10^{10}$ N/ m^2	Piezoelectric constant e_{15} C/ m^2	Permittivity ε_{11} 10^{-11} F/m	Density ρ 10^3 kg/ m^3
PZT-4	2.56	12.7	646	7.6
$LiIO_3$	1.78	0.89	6.434	3.402
$BaTiO_3$	5.43	11.6	1744	6.02

Fig. 3 shows wave trapping for the lowest mode for a $BaTiO_3$ and $LiIO_3$ waveguide, where the horizontal lines show the cut-off frequencies in two materials. The nature of the trapping is the same as that described in detail in Piliposyan et al. (2014). For a waveguide with short thin cells ($\beta < h$) the mode is localized near the interfaces between the two materials for all values of the reduced wave number (Fig.3a). As the length of the unit cell increases compared to the waveguide height (Fig.3b) the dispersion curves for the piezoelectric waveguide become flatter. Due to a large difference between the acoustic impedances of $BaTiO_3$ and $LiIO_3$ the frequency

region of the piezoelectric waveguide with trapped waves is large and for longer cells includes several modes (Fig. 3b).

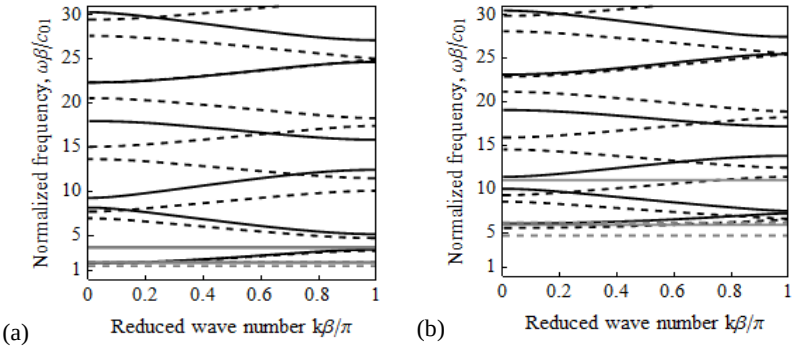

Fig. 3. Band structure for a $LiIO_3$ and $BaTiO_3$ piezoelectric phononic crystal for $n=1$ (a) β/h=0.5, (b) β/h=1.5. Solid lines and dashed lines show the band structure with and without the piezoelectric effect, horizontal lines show the cut-off frequencies in the two materials.

The transmission coefficients in Fig. 4 confirm the above results, showing full reflection when the Bragg resonance conditions are satisfied (i.e., when the value of the wave number lies inside the forbidden zones of the Bloch spectrum) and the number of layers is sufficiently large.

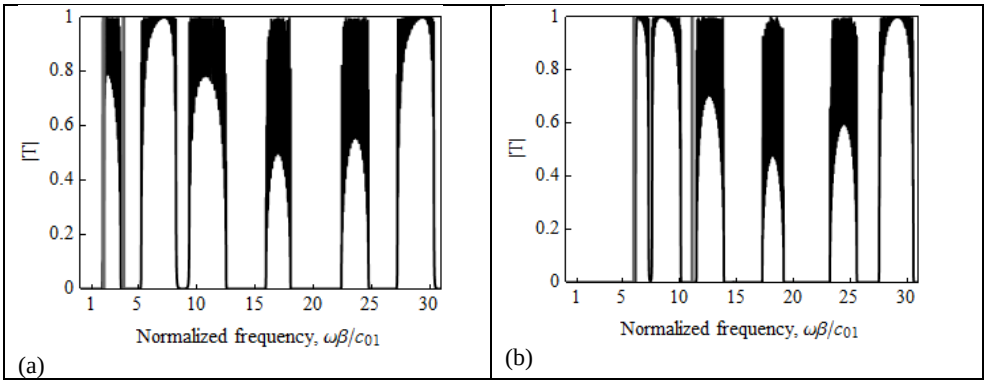

Fig. 4. Absolute value of the transmission coefficient for a $LiIO_3$ and $BaTiO_3$ piezoelectric phononic crystal for (a) β/h=0.5, (b) β/h=1.5, M=50. Vertical gray lines show the cut-off frequencies in each material.

A superlattice made up of a unit cell with identical PZT-4 material also demonstrates frequency gaps and increasing cut-off frequencies for longer unit cells (Fig.5a,b). The frequency gaps in this case are only in the middle of the Brillouin zone, where the first gap remains always the largest, and as can be seen also from the reflection coefficient (Fig. 6) does not have significant change in its width.

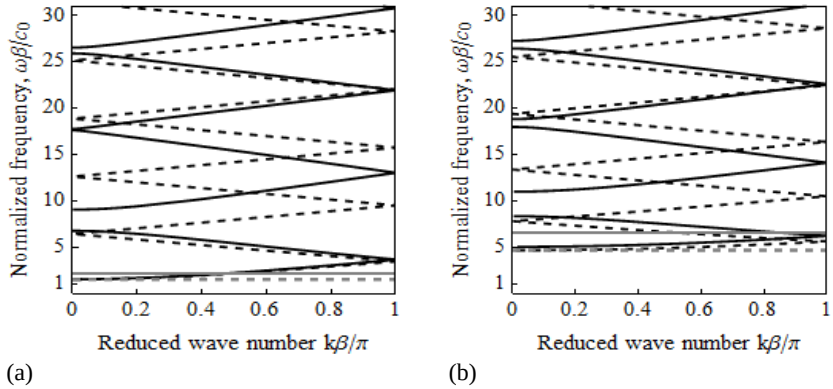

Fig. 5. a) Superlattice with identical PZT-4 crystals in both layers of the unit cell a) $\beta/h=0.5$, b) $\beta/h=1.5$. Dashed lines show the band structure without piezoelectric effect, horizontal lines show the cut-off frequencies

Another interesting feature here is that the Bloch wave number can have a real value below the cut off frequency. This is better shown for longer unit cells (Fig 5b.) and does not happen when the piezoelectric effect is neglected. This can also be shown analytically from the dispersion equation (28) where below cut off acoustic frequencies $\omega^2/c_0^2 - p^2 < 0$ and $\omega^2/c^2 - p^2 < 0$. If we expand the right hand side of (28) as a series with respect to a small parameter θ, the first term of series is

$$F(\omega) = \cos(aq) + \theta \frac{p^2}{qs} \frac{\sin(aq)}{\sin(as)} \left(\cos(as) - \cos(aq)\right).$$

Since $F(0) = \cosh(\pi\beta/h) > 1$, it follows that there is not propagating mode. At the cut-off frequency $\omega_0 = c_0 p/h$, taking into account that $(c_0/c)^2 << 1$, $F(\omega_0)$ can be approximated as $1 - \theta a_0 \pi \tanh(a_0\pi/2) < 1$. This means that there exists a region below the cut-off frequency where the waveguide supports an evanescent mode.

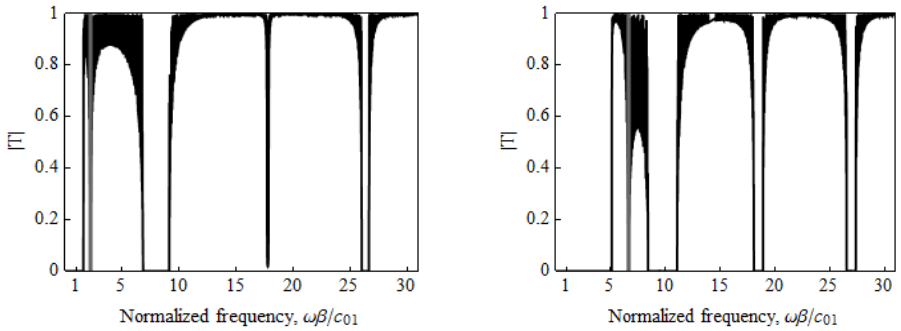

(a) (b)

Fig. 6. Absolute value of the transmission coefficient for a superlattice with identical PZT-4 crystals in both layers of the unit cell (a) β/h=0.5, (b) β/h=1.5, M=100. Vertical gray lines show the cut-off frequency.

Due to the fixed electro-potential condition, a superlattice with identical elements in the unit cell demonstrates a much sharper resonant enhancement of transmission (Fig. 6). In this case each interface provides a reflection proportional to only the electromechanical coupling parameter θ<1 (Alshits and Shuvalov, 1995) and near the Bragg resonance, where $|T| = 0$ for a sufficiently large number of layers, the transmission coefficient experiences a sharp decrease compared to waveguides with a unit cell made of different piezoelectric materials (Fig. 4).

4.2 Periodically alternating boundary conditions

The transfer matrices (19) can also be used to solve the problem for piezoelectric waveguides with straight parallel boundaries imposed by alternating boundary conditions on the waveguide walls. If the lower wall is displacement-clamped and electrically-shorted ($u = 0$, $E_x = 0$) and the upper wall traction-free and magnetically-closed ($\sigma_{yz} = 0$, $H = 0$) the modes again separate and the problem is described by the dispersion equation (27) for all modes including mode $n = 0$.

Calculations have been made for a $LiIO_3$ and $BaTiO_3$ phononic crystal which is displacement-clamped and electrically-shorted on the lower wall and traction-free and magnetically-closed on the upper wall in the first layer of the unit call, and vice versa in the second layer. The qualitative behavior of the wave propagation without the piezoelectric effect is similar to that for the waveguide with full contact interfacial conditions discussed in detail in Piliposyan et al. (2014). For short cell lengths $(\beta/h = 0.5)$ without the piezoelectric effect there is only a zero frequency cut off and no other band gaps. As the cell length increases ($\beta/h = 1.5$) the modes start mixing, the zero frequency cut offs appear at higher frequencies and stop band gaps appear with a clear minimum within the Brillouin zone indicating the existence of slow waves (Piliposyan et al., 2014).

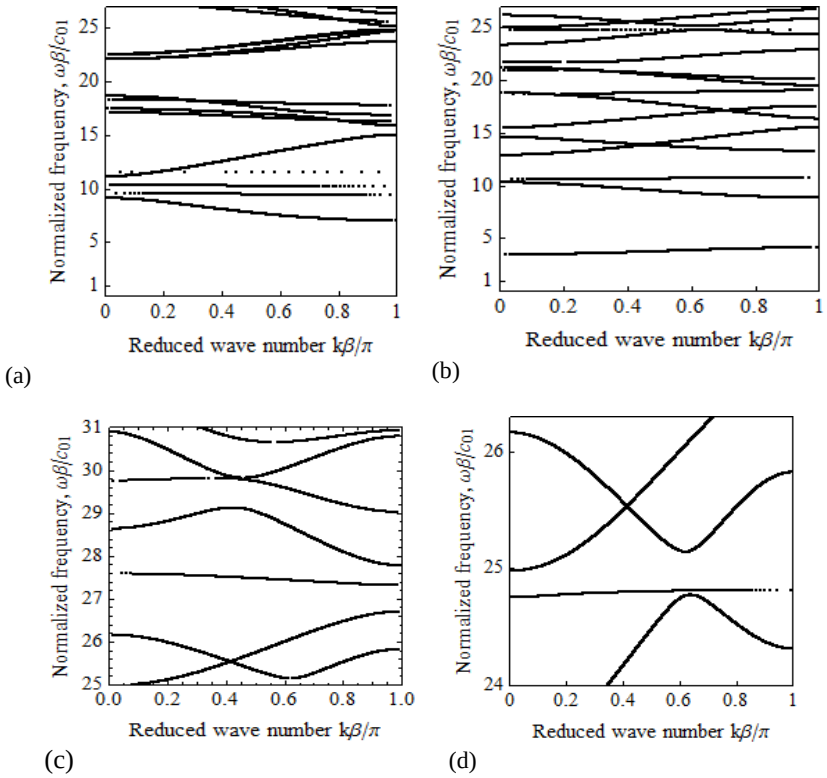

Fig. 7. Band structure for a $LiIO_3$ and $BaTiO_3$ phononic crystals with $u = 0$, $E_x = 0$ on the lower wall and $\sigma_{yz} = 0$, $H = 0$ on the upper wall of the first material and vice versa in the second material a) $\beta / h = 0.5$ (b),(c),(d) $\beta / h = 1.5$.

For the piezoelectric waveguide, even for short cell lengths there is a zero frequency cut-off followed by a wide band gap (Fig.7a). Two completely flat curved within the first gap indicate standing waves with no propagating energy and this is associated with mode trapping. With the aspect ratio β/h increasing the modes mix up, the first cut-off frequency increases and one of the flat curves stays well below the cut-off frequency. As the detailed pictures show (Fig. 7c, 7d) this mode mixing causes more trapped modes occurring within higher frequency gaps.

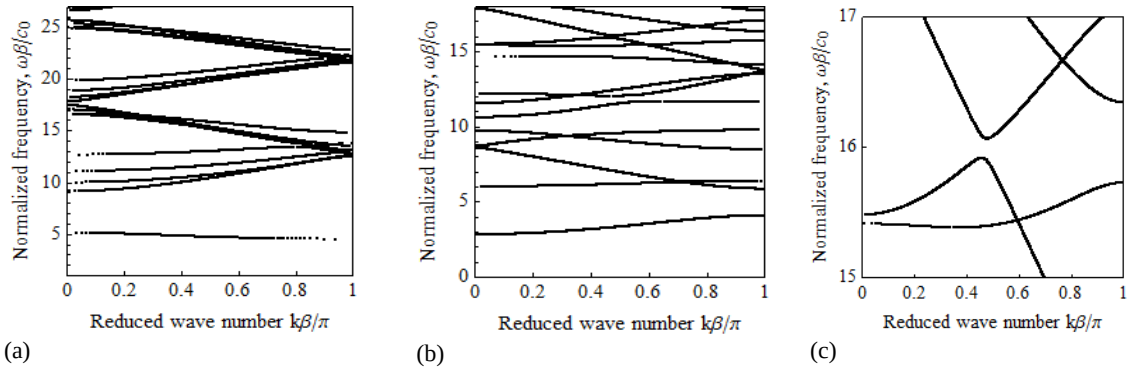

Fig. 8. Band structure for PZT-4 phononic crystals with $u=0$, $E_x=0$ on the lower wall and $\sigma_{yz}=0$, $H=0$ on the upper wall of the first material and vice versa in the second material, a) $\beta/h=0.5$ (b),(c) $\beta/h=1.5$.

The effect of the alternating boundary conditions on the waveguide walls on wave trapping are more visible for a piezoelectric waveguide with identical elements in the unit cell. For small values of β/h there are band gaps only in the middle of the Beryllium zone (Fig. 8a). The flat curve corresponding to standing waves with very little propagating energy occur below the first cut-off frequency. With larger values of β/h the cut-off frequency increases leaving below two slow modes. At higher frequencies the folding of modes causes modes crossing and opening of band gaps at the edge of Brillouin zone (Fig.8b) or stop band gaps appear with a clear minima within the Brillouin zone.

4.3 Tuneable passband in the piezoelectric composite waveguide

We now use the transmission coefficient (45) to investigate the transmission properties of SH waves in the piezoelectric waveguide with a defect layer (Fig. 2).

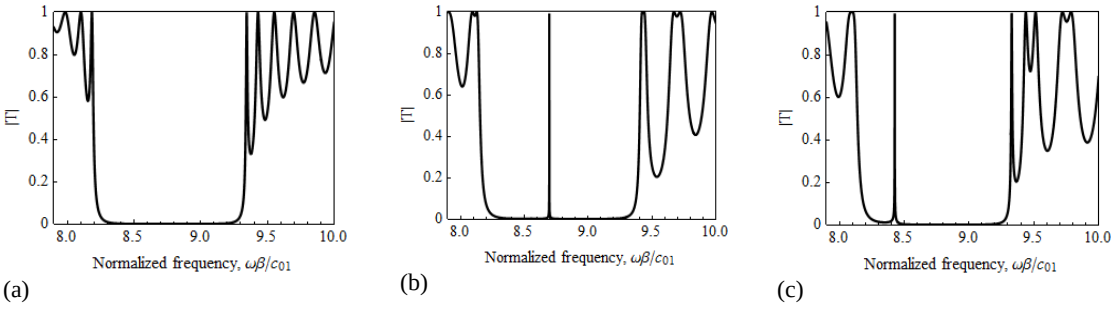

Fig. 9. Absolute values of the transmission coefficient for a $LiIO_3$ and $BaTiO_3$ piezoelectric phononic crystal with displacement-clamped and electrically-shorted boundaries on the guide walls for β/h=0.5, M=25 (a) without a defect layer, (b)with a defect layer with thickness $d_c=\beta$, (c) with a defect layer with thickness $d_c=1.5\beta$.

Fig. 7 compares the transmission spectrum of the piezoelectric composite waveguide $LiIO_3$ and $BaTiO_3$ with and without a defect layer. Without a defect layer (Fig.9a) a typical propagation feature with an acoustic bandgap is observed. The presence of a defect layer, which has material parameters of LiIO3 without a piezoelectric effect, (Figs.9b & 9c) shows broadening

of the forbidden band. Further, a passband with a transmission peak of 100% appears within the bandgap. Increasing the thickness of the defect layer from $d_c = \beta$ (Fig.9b) to $d_c = 1.5\beta$ (Fig.9c) moves the passband from $\omega\beta / c_{01} = 8.7$ to $\omega\beta / c_{01} = 8.4$, demonstrating that the passband can be tuned by changing the thickness of the defect layer.

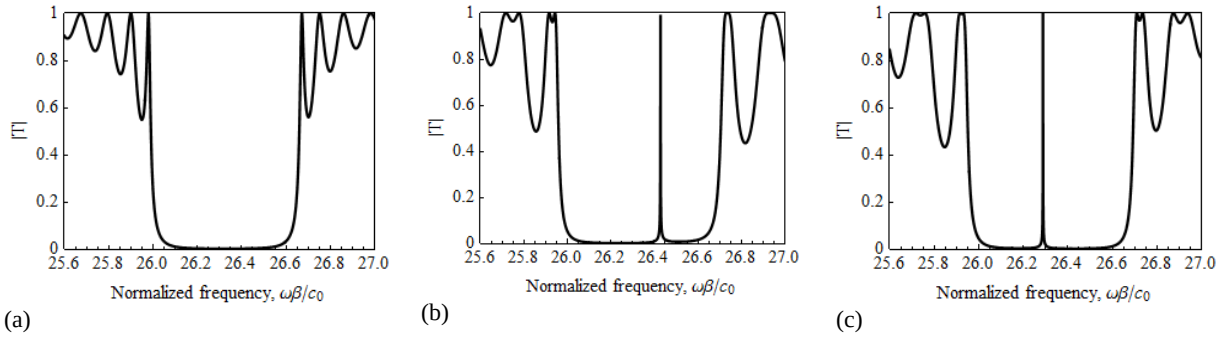

Fig. 10. Absolute values of the transmission coefficient identical PZT-4 crystals in both layers of the unit cell with displacement-clamped and electrically-shorted boundaries on the guide walls for β/h=0.5, M=25, (a)without a defect layer, (b)with a defect layer with thickness $d_c = \beta$, (c) with a defect layer with thickness $d_c = 1.5\beta$.

Fig. 10 shows similar results for a piezoelectric waveguide with cells composed of an identical piezoelectric material PZT-4. The transmission spectrum for a waveguide without a defect layer is shown in Fig. 10a. Figs. 10b &10c show that the presence of a defect layer, which has material parameters of PZT-4 without a piezoelectric effect, results in a slight broadening of the bandgap and the appearance of a 100% transmission passband within the bandgap. Changing the thickness of the defect layer from $d_c = \beta$ (Fig.10b) to $d_c = 1.5\beta$ (Fig.10c) moves the passband from $\omega\beta / c_{01} = 2.263$ to $\omega\beta / c_{01} = 2.262$ though in this case without changing the width of stopband.

5. Conclusion

The propagation of elasto-electromagnetic coupled SH waves in a quasi-one dimensional periodic piezoelectric waveguide with metallized interfaces is considered in this paper. The complete dispersion relation with perfectly matched physical fields at the interfaces is described by two coupled equations and include information about a coupled elasto-electromagnetic wave and acousto-optic resonances called phonon-polariton (Piliposyan et al., 2014). Without the piezoelectric effect the two equations decouple, one describing the propagation of an electromagnetic wave in a photonic crystal and the other an acoustic wave in a phononic crystal.

In the case when there are not full interfacial contacts the wave process is described by only one dispersion relation which in the absence of the piezoelectric effect describes the propagation of only one acoustic wave in a phononic crystal. In this case only one coupled

electro-elastic wave propagates in the system combining both elastic and electro-magnetic effects.

The structure of wave propagation strongly depends on the ratio of the length of the unit cell to the height of the waveguide β/h and differences between the elastic and electromagnetic properties of the piezoelectric layers.

When the unit cell in the waveguide is made from two different constituent materials, wave trapping occurs with the waves exponentially decaying in one layer, creating a stop band below the lowest of the two cut-off frequencies where no propagation is possible.

In the case of electrically shorted interface conditions band gaps exist also when the constituent materials in the cells of the waveguide are identical. In this case the periodic system becomes a periodic system of interfaces where the magnetic field intensity experiences discontinuity. There is only one cut-off frequency and instead of trapping there are evanescent modes propagating below the cut-off frequency. The reflection of an electro-elastic wave is caused by the equipotential condition on the interfaces. Since the parameter of electromechanical coupling is normally very small, the reflection coefficient experiences a sharp increase near the resonances providing sharpening of certain properties compared to periodic structure made from different piezoelectric layers with both metallised and non-metallized interfaces.

Alternating boundary conditions on the waveguide walls for a piezoelectric waveguide with straight parallel boundaries introduce new effects and opens a possibility for new developments in the design of stopband acoustic homogeneous guides in which stopbands occur only due to alternating conditions on the walls. The existence of completely flat curves within the frequency gaps indicate standing waves with no propagating energy and this is associated with mode trapping. The results show situations where the stopbands achieve minimum values for the Bloch parameter strictly within the first Brillouin zone. This is related to the phenomenon of slow waves (Figotin and Vitebskiy, 2006) and in this case periodic guides with boundary perturbations exhibiting this behaviour can be easily constructed. These have many important potential applications, including for example improved elastic delay lines.

Controlling wave propagation properties including slowing down the propagation of light or sound or creating passband inside the stopband is also possible by introducing some disorder in periodically layered structures. We have found an analytical expression for the transmission coefficient that can be used to accurately detect the position of the passband inside a stopband. This can have applications in designing tunable waveguides which can even be made of layers of identical piezoelectric crystal separated by metallized interfaces.

Acknowledgments

This research was supported by the State Committee of Science of Armenia Grant No. SCS 115T-2C031.

References

Achaoui, Y., Khelif, A., Benchabane, S., Laude V., 2010. Polarisation state and level repulsion in two-dimensional phononic crystals and waveguides in the presence of material anisotropy. J. of Phys. D: Appll. Phys. 43, 185401.

Adams, S.D.M., Craster, R.V., Guenneau, S., 2008. Bloch waves in periodic multi-layered acoustic waveguides. Proc. R. Soc. A 464, 2669-2692.

Adams, S.D.M., Craster, R.V., Guenneau, S., 2009. Guided and standing Bloch waves in periodic elastic strips. Waves Rand. Compl. Media 19(2): 321–346.

Alshits, V.I., Gorkunova, A.S., Shuvalov, A.L., 1996. Phase resonance in the reflection of acoustic waves by a system of piezocrystalline layers separated by cladding layers with screening properties. J. Exp. Theor. Phys. 83, 509-516.

Alshits, V.I., Shuvalov, A.L., 1995. Resonance reflection and transmission of shear elastic waves in multilayered piezoelectric structures. J. Appl. Phys. 77 (6), 2659-2665.

Belubekyan M.V., 2008. Screen surface shear wave in a piezo-active semi-space of hexagonal symmetry, Proc. 6th Int. Conf., Problems of Dynamics of Interaction of Deformable Media, 125-130.

Craster, R.V., Guenneau, S., Adams, S.D.M., 2009. Mechanism for slow waves near cutoff frequencies in periodic waveguides. Phy. Rev. B 79, 045129.

Darinskii A. N., Le Clezio E., Feuillard G., 2008. Electromagnetic surface wave attenuation caused by acoustic wave radiation. Electromagnetics 28, 175-185.

Darinskii A. N., Le Clezio E., Feuillard G., 2008. The role of electromagnetic waves in the reflection of acoustic waves in piezoelectric crystals. Wave Motion 45, 428-444.

Darinskii, A. N., Le Clezio, E., Feuillard G., 2007. Acoustic waves in the vicinity of the normal to the surface of piezoelectric crystals. IEEE Trans. Ultrason., Ferroelect., Freq. Contr. 54(4), 612-620.

Figotin, A., Vitebskiy, I., 2006. Slow light in photonic crystals. Waves Rand. Compl. Media 16, 293–392.

Ghazaryan, K.B., Piliposyan, D.G., 2012. Interfacial effects for shear waves in one dimensional periodic piezoelectric structure. J. Sound Vib., 330(26), 6456-6466.

Goffaux, C., Vigneron, J.P., 2011. Theoretical study of a tunable phononic band gap system. Phys. Rev. B: Condens. Matter 64, 075118.

Guo, Y., Chen, W., Zhang, Y, 2009. Guided wave propagation in multi-layered piezoelectric structures. Sci. China Ser. G: Phys., Mech. &Astr. 52(7), 1094-1104.

Piliposyan D.G., Ghazaryan K.B., Piliposian G.T., 2015. Magneto-electro–elastic polariton coupling in a periodic structure. J. Phys. D: Appl. Phys. 48 (2015) 175501.

Piliposian, G.T., Avetisyan, A.S., Ghazaryan, K.B., 2012. Shear wave propagation in periodic phononic/photonic piezoelectric medium. Wave Motion 49(1):125-134.

Piliposyan, D.G., Ghazaryan, K.B., Piliposian, G.T., 2014. Shear Bloch waves and coupled phonon–polariton in periodic piezoelectric waveguides. Ultrasonics 54(2), 644–654.

Postnova, J., Craster, R.V., 2007. Trapped modes in topographically varying elastic waveguides. Wave Motion 44, 205–221.

Sabina, F.J., Movchan, A.B., 2009. Interfacial effects in electromagnetic coupling within piezoelectric phononic crystals. Acta Mech. Sin., 25, 95-99.

Sugimoto, M., Makimoto, T., 1973. Analysis of mode coupling in piezoelectric waveguides. Appl. Phys., 45(4),1643-1649.

Vashishth, A.K, Gupta, V., 2009. Wave propagation in transversely isotropic porous piezoelectric materials. Int. J. Solids Struct. 46, 3620–3632.

Wang, Y.Z., Li F.M., Kishimoto, K., Wang, Y.S., Huang, W.H., ,2009. Wave band gaps in three-dimensional periodic piezoelectric structures. Mech. Research Comm. 36, 461–468.

Wilm, M., Ballandras, S., Laude, V., Pastureaud, T., 2002. A full 3D plane-wave expansion model for 1-3 piezoelectric composite structures. J. Acous. Soc.Amer. 112, 943–952.

Yan, Z.Z., Wang, Y.S., 2008. Calculation of band structures for surface waves in two dimensional phononic crystals with a wavelet-based method. Phys. Rev. B 78, 094306.

Zou, X.Y., Chen, Q., Liang, B., Cheng, J.C., 2008. Control of the elastic wave band gaps in two-dimensional piezoelectric periodic structures. Sm. Mat. Struct. 17, 015008.